

Continuum of Bound States in a Non-Hermitian Model

Qiang Wang¹, Changyan Zhu¹, Xu Zheng¹, Haoran Xue¹, Baile Zhang^{1,2,*} and Y. D. Chong^{1,2,†}

¹*Division of Physics and Applied Physics, School of Physical and Mathematical Sciences, Nanyang Technological University, Singapore 637371, Singapore*

²*Centre for Disruptive Photonic Technologies, Nanyang Technological University, Singapore 637371, Singapore*

 (Received 18 October 2022; accepted 14 February 2023; published 8 March 2023)

In a Hermitian system, bound states must have quantized energies, whereas free states can form a continuum. We demonstrate how this principle fails for non-Hermitian systems, by analyzing non-Hermitian continuous Hamiltonians with an imaginary momentum and Landau-type vector potential. The eigenstates, which we call “continuum Landau modes” (CLMs), have Gaussian spatial envelopes and form a continuum filling the complex energy plane. We present experimentally realizable 1D and 2D lattice models that host CLMs; the lattice eigenstates are localized and have other features matching the continuous model. One of these lattices can serve as a rainbow trap, whereby the response to an excitation is concentrated at a position proportional to the frequency. Another lattice can act a wave funnel, concentrating an input excitation onto a boundary over a wide frequency bandwidth. Unlike recent funneling schemes based on the non-Hermitian skin effect, this requires a simple lattice design with reciprocal couplings.

DOI: [10.1103/PhysRevLett.130.103602](https://doi.org/10.1103/PhysRevLett.130.103602)

The bound states of a quantum particle in an infinite continuous space have energies that are quantized [1,2]. This stems from a theorem that compact Hermitian Hamiltonians have pure point spectra [3–5], and accounts for the energy quantization in standard models such as the harmonic oscillator and potential well [6]. The principle also applies to Anderson localized states in random potentials, whose eigenenergies are dense but countable [7,8], and to the long-wavelength regime of discrete (e.g., tight-binding) lattices [9–14]. Free states, by contrast, are spatially extended and form continuous spectra. It is interesting to ask whether any physical system could behave differently, such as having an uncountable set of bound states. How might such a Hamiltonian be realized, and what interesting properties might its eigenstates have?

Over the past two decades, a large body of literature has developed around the study of non-Hermitian Hamiltonians [15–22], catalyzed by the realization that such Hamiltonians can be implemented on synthetic classical wave structures such as photonic resonators and waveguide arrays [23–27]. Non-Hermitian systems have been found to exhibit various interesting and useful features with no Hermitian counterparts. For instance, their spectra can contain exceptional points corresponding to the coalescence of multiple eigenstates [28–32], which can be used to enhance optical sensing [33–35]. Another example is the non-Hermitian skin effect, whereby a non-Hermitian lattice’s eigenstates condense onto its boundaries [36–45], with possible applications including light funneling [46] and the stabilization of laser modes [47,48].

This raises the possibility of using non-Hermitian systems to violate the standard distinctions between

quantized bound states and continuous free states, which were derived under the assumption of Hermiticity [49]. Here, we investigate a non-Hermitian Hamiltonian that has spatially localized energy eigenstates, which we call “continuum Landau modes” (CLMs), at every complex energy E . The Hamiltonian features a first-order *imaginary* dependence on momentum, along with a Landau-type vector potential [6]; its eigenstates, the CLMs, map to the zero modes of a continuous family of Hermitian 2D Dirac models [50–55]. In two dimensions (2D), the CLM’s center position \mathbf{r}_0 varies linearly and continuously with the complex plane coordinates of E . By contrast, previous studies of non-Hermitian models with vector potentials found only quantized bound states, similar to the Hermitian case [56–58]. We moreover show that the desired Hamiltonian arises in the long-wavelength limit of a 2D lattice with nonuniform complex mass and nonreciprocal hoppings [40,43–45], which can be realized experimentally with photonic structures [59,60] or other classical wave metamaterials [46,61–67]. If the lattice size is finite, the CLMs become countable but retain other key properties like the dependence between \mathbf{r}_0 and E .

One dimensional (1D) versions of the model can be realized in lattices with nonuniform real mass and nonreciprocal hoppings, with the CLM positions proportional to $\text{Re}(E)$; or nonuniform imaginary mass and reciprocal hoppings, with CLM positions proportional to $\text{Im}(E)$. The first type of lattice can act as a non-Hermitian rainbow trap [68–71], in which excitations induce intensity peaks at positions proportional to the frequency. Compared to a recent proposal for rainbow trapping using topological states within a band gap [70,71], the CLM-based rainbow

trapping scheme has the potential to operate over a wide frequency bandwidth. The second type of 1D lattice acts as a wave funnel [46]: the response to an excitation is concentrated at one boundary. This is similar to the funneling caused by the non-Hermitian skin effect [46], but requires only the placement of on-site gain or loss without nonreciprocal couplings, and may therefore be easier to implement [72–75].

We begin by reviewing Landau quantization in 2D Hermitian systems. As shown in Fig. 1(a), a free non-relativistic particle has a continuum of extended (free) states with a quadratic energy dispersion, and when a uniform magnetic field is applied, the spectrum collapses into a discrete set of Landau levels [6]. For a Dirac particle with a linear dispersion relation, a magnetic field likewise produces a discrete spectrum [50–52,76], as shown in Fig. 1(b). With appropriate gauge choices, the Landau levels are spanned by normalizable eigenfunctions (bound states) interpretable as cyclotron orbits.

Now consider the non-Hermitian 2D Hamiltonian

$$\mathcal{H} = s_x \left[-i \frac{\partial}{\partial x} - By \right] + is_y \left[-i \frac{\partial}{\partial y} + Bx \right], \quad (1)$$

where $s_{x,y} = \pm 1$ (these are scalars, not matrices). For $B = 0$, this kind of “non-Hermitian Dirac Hamiltonian” has recently been analyzed in studies of non-Hermitian band topology [77,78]; its spectrum is given by $E_0(\mathbf{k}) = s_x k_x + is_y k_y$, as shown in Fig. 1(c). The $B \neq 0$ case introduces a symmetric-gauge vector potential corresponding to a uniform out-of-plane magnetic field $2B\hat{z}$, via the substitution $-i\nabla \rightarrow -i\nabla + \mathbf{A}$. The eigenstates of \mathcal{H} are

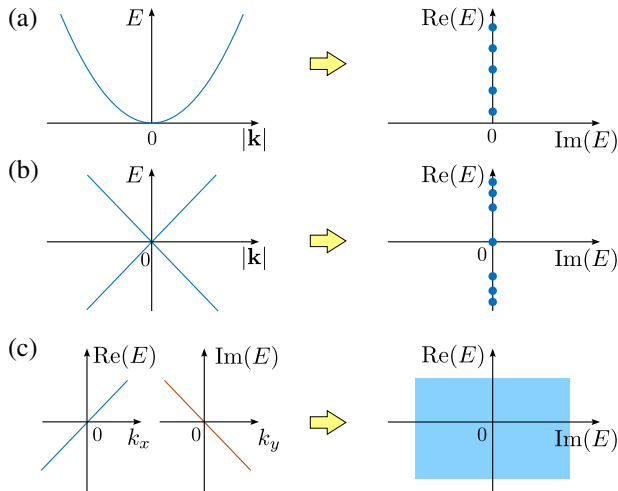


FIG. 1. Effects of a uniform magnetic field on the spectra of 2D models. (a) For a nonrelativistic particle with quadratic dispersion, the spectrum collapses into discrete Landau levels. (b) For a Dirac particle, the spectrum forms an unbounded sequence of Landau levels. (c) For the non-Hermitian Hamiltonian (1), the complex linear dispersion relation turns into a continuum of bound states filling the complex energy plane.

$$\psi(x, y) = C \exp[-\tau |\mathbf{r} - \mathbf{r}_0|^2 + i\mathbf{q} \cdot \mathbf{r}], \quad (2)$$

$$\mathbf{r}_0(E, \mathbf{q}) = \frac{1}{B} \begin{pmatrix} \text{Im}[E - E_0(\mathbf{q})]/s_y \\ -\text{Re}[E - E_0(\mathbf{q})]/s_x \end{pmatrix}, \quad (3)$$

where C is a normalization constant, $\tau = -s_x s_y B/2$, $\mathbf{q} = (q_x, q_y)$ is an arbitrary real vector, and E is the eigenenergy. If $\tau > 0$, the wave functions are normalizable on \mathbb{R}^2 regardless of E and \mathbf{q} , with characteristic length $\ell \sim B^{-1/2}$. The eigenenergies fill the complex plane, as shown in Fig. 1(c). For each E , there is a continuum of bound states centered at different \mathbf{r}_0 , via Eq. (3); also, states with the same \mathbf{q} but different \mathbf{r}_0 are nonorthogonal. Note that such a continuum is not a generic consequence of non-Hermiticity; other recently studied non-Hermitian models incorporating uniform magnetic fields exhibit the usual quantized spectra [57,58].

We call these eigenstates CLMs because they are closely related to zeroth Landau level (OLL) modes of massless 2D Dirac fermions [50–55]. CLMs with a given energy E have a one-to-one map with the OLL modes of a given Hermitian Dirac Hamiltonian, whose gauge is determined by E . The full set of CLM eigenstates for \mathcal{H} thus maps to the OLL modes of a *family* of Dirac Hamiltonians with different gauges, and the CLMs are uncountable because the gauge can be continuously varied. For details about this mapping, including the role of gauge invariance, see Supplemental Material [49].

Because of the localization of the CLMs, wave functions resist diffraction when undergoing time evolution with \mathcal{H} . For instance, a Gaussian wave packet maintains its width under time evolution (even if the width differs from that of the CLMs); however, depending on the initial settings, the wave packet can move and undergo amplification or decay, as detailed in Supplemental Material [49].

CLMs can also be observed in the continuum limit of discrete lattices. Take the 2D lattice depicted in Fig. 2(a), whose Hamiltonian is

$$\mathcal{H} = \sum_{\mathbf{r}} [B(y - ix)a_{\mathbf{r}}^{\dagger}a_{\mathbf{r}} + t_x(a_{\mathbf{r}-\hat{x}}^{\dagger}a_{\mathbf{r}} + \text{H.c.}) + t_y(a_{\mathbf{r}-\hat{y}}^{\dagger}a_{\mathbf{r}} - \text{H.c.})], \quad (4)$$

where $a_{\mathbf{r}}^{\dagger}$, $a_{\mathbf{r}}$ are creation and annihilation operators at $\mathbf{r} = (x, y) \in \mathbb{Z}^2$ (the lattice constant is set to 1), and $t_x, t_y \in \mathbb{R}$ are hopping coefficients. \mathcal{H} is non-Hermitian due to the imaginary part of the mass and the nonreciprocity of the y hoppings [40,43–45]. Such nonreciprocal hoppings can be realized on experimental platforms such as circuit lattices, fiber loops, and ring resonator lattices [46,61–67], which have notably been used to study the non-Hermitian skin effect [36,37,40,41,43–45]. Note, however, that this lattice does not exhibit the skin effect [49].

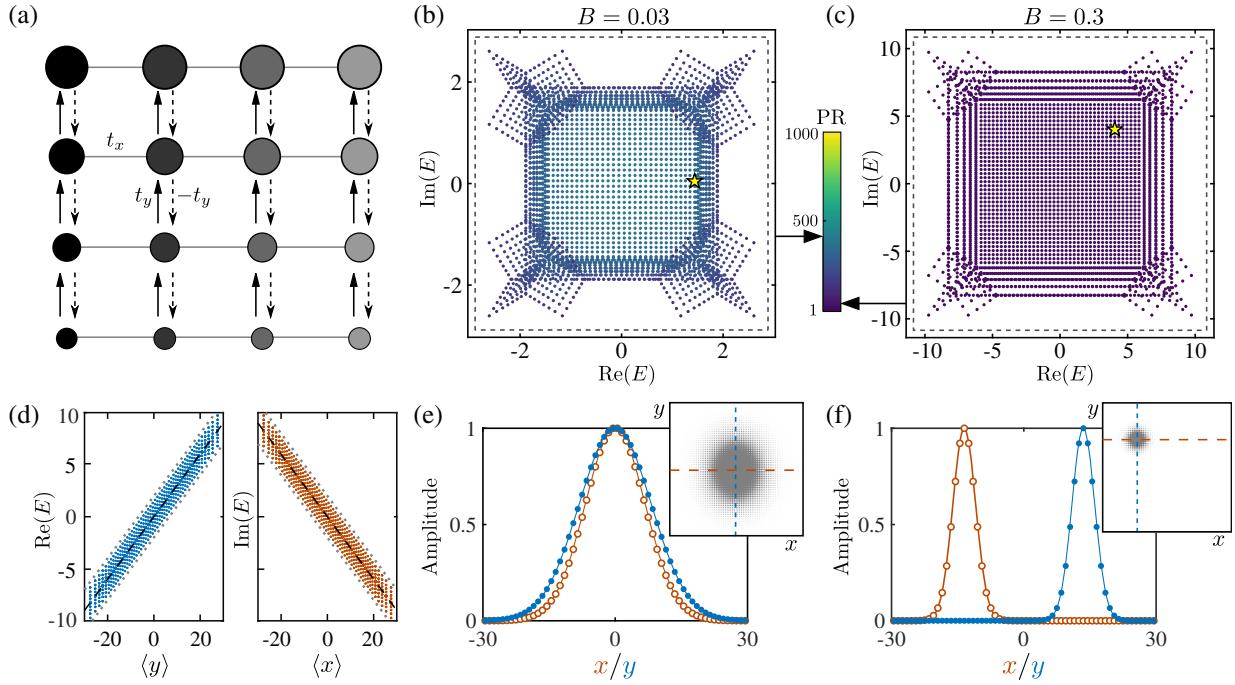


FIG. 2. Continuum Landau modes (CLMs) in a 2D lattice. (a) Schematic of a square lattice with reciprocal hoppings along x (gray lines), nonreciprocal hoppings along y (black arrows), and on-site mass $m_{x,y} = B(y - ix)$ (size and darkness of the circles indicate the real and imaginary parts). (b),(c) Complex energy spectra for finite lattices with (b) $B = 0.03$ and (c) $B = 0.3$. The color of each dot corresponds to the participation ratio (PR) of the eigenstate; a more localized state has lower PR. The arrows on the color bar indicate the highest PR for the CLM ansatz, for each B . The dashed boxes are the bounds on CLM eigenenergies derived from Eq. (7). (d) Plot of $\text{Re}(E)$ versus $\langle y \rangle$ (left panel) and $\text{Im}(E)$ versus $\langle x \rangle$ (right panel) for $B = 0.3$. The black dashes and gray dotted lines, respectively, indicate the theoretical central trend line (corresponding to $E_{\mathbf{k}+\mathbf{q}}^0 \rightarrow 0$) and bounding lines derived from Eq. (7). (e),(f) Wave function amplitude $|\psi_{\mathbf{r}}|$ for the eigenstates marked by yellow stars in (b) and (c), respectively. Hollow and filled circles, respectively, indicate the variation with x and y , along lines passing through the center of each Gaussian; solid curves show the CLM predictions. Insets show the distribution in the 2D plane. In (b)–(f), we use $t_x = t_y = 1$ and a lattice size of 60×60 , with open boundary conditions.

For $B = 0$, \mathcal{H} has discrete translational symmetry and dispersion relation $E_{\mathbf{k}}^0 = 2(t_x \cos k_x + it_y \sin k_y)$, where $k_{x,y} \in [-\pi, \pi]$. Taking $|\psi_{\mathbf{k}}\rangle = \sum_{\mathbf{r}} \exp(i\mathbf{k} \cdot \mathbf{r}) \Psi_{\mathbf{r}} a_{\mathbf{r}}^{\dagger} |\emptyset\rangle$, where $|\emptyset\rangle$ is the vacuum state, the slowly varying envelope obeys $H_{\mathbf{k}} \Psi_{\mathbf{r}} = E \Psi_{\mathbf{r}}$, where [49]

$$H_{\mathbf{k}} = E_{\mathbf{k}}^0 - \left[-i\mu_{\mathbf{k}} \frac{\partial}{\partial x} - By \right] + i \left[-i\nu_{\mathbf{k}} \frac{\partial}{\partial y} - Bx \right], \quad (5)$$

$$\mu_{\mathbf{k}} = 2t_x \sin k_x, \quad \nu_{\mathbf{k}} = 2t_y \cos k_y, \quad (6)$$

to first order in spatial derivatives. Note that the complex masses in (4) produce the pseudovector potential [50–55]. For $B/\mu_{\mathbf{k}} < 0$, $B/\nu_{\mathbf{k}} > 0$, there exist CLMs similar to (2), with τ replaced by $\tau_x = -B/2\mu_{\mathbf{k}}$, $\tau_y = B/2\nu_{\mathbf{k}}$, and Eq. (3) replaced by

$$\mathbf{r}_0(E, \mathbf{k}, \mathbf{q}) = \frac{1}{B} \begin{pmatrix} -\text{Im}(E - E_{\mathbf{k}+\mathbf{q}}^0) \\ \text{Re}(E - E_{\mathbf{k}+\mathbf{q}}^0) \end{pmatrix} + O(|\mathbf{q}|^2). \quad (7)$$

As $\Psi_{\mathbf{r}}$ is assumed to vary slowly in \mathbf{r} , the solutions are limited to the regime $|\mathbf{q}| \ll 1$. If the lattice is infinite, they

form a continuous set spanning all $E \in \mathbb{C}$. For a finite lattice, the eigenstates are finite and hence countable, and the CLMs reduce to a band over a finite area in the E plane. In Figs. 2(b) and 2(c), we plot the spectra for $B = 0.03, 0.3$, each lattice having size $L_x = L_y = 60$, open boundary conditions, and $t_x = t_y = 1$. By requiring \mathbf{r}_0 to lie in the lattice, Eq. (7) implies the bounds $|\text{Re}(E)| \lesssim BL_y/2 + 2t_x$ and $|\text{Im}(E)| \lesssim BL_x/2 + 2t_y$. For large $L_{x,y}$, the energy discretization is of order B .

All of the numerically obtained eigenstates are CLMs. The color of each data point in Figs. 2(b) and 2(c) indicates the participation ratio (PR), defined for a wave function $\psi_{\mathbf{r}} = \langle \mathbf{r} | \psi \rangle$ as $\langle \psi | \psi \rangle^2 / \sum_{\mathbf{r}} |\langle \mathbf{r} | \psi \rangle|^4$, with large PR (of order N^2) corresponding to extended states [79]. We find that all eigenstates have PR consistent with the CLM predictions, and well below N^2 (for each case, the maximum PR, attained when $|\mu_{\mathbf{k}}| = |\nu_{\mathbf{k}}| = 1$, is indicated by an arrow in the color bar). Figure 2(d) plots each eigenstate's energy against the position expectation values $\langle x \rangle$ and $\langle y \rangle$, for $B = 0.3$. This reveals the linear relationship between E and \mathbf{r}_0 predicted in Eq. (7) (indicated by dashes), and the upper and lower bounds introduced by the $E_{\mathbf{k}+\mathbf{q}}^0$

lines). Figures 2(e) and 2(f) compare the spatial amplitude $|\psi_{\mathbf{r}}|$ for two arbitrarily chosen numerical eigenstates to the CLM solutions, which are in good agreement.

CLMs can also be realized in 1D lattices, which are simpler to implement experimentally. We study two kinds of lattices, which have different behaviors.

The first 1D lattice, shown in Fig. 3(a), has a real mass gradient and nonreciprocal hoppings. Its Hamiltonian is

$$\mathcal{H} = \sum_j [B(j - j_0)a_j^\dagger a_j + ta_j^\dagger a_{j-1} - ta_{j-1}^\dagger a_j], \quad (8)$$

where $B, t \in \mathbb{R}$. For a finite lattice with $1 \leq j \leq N$, we take $j_0 = \frac{1}{2}(N + 1)$. The nonreciprocal nearest neighbor hoppings $\pm t \in \mathbb{R}$ are indicated by solid and dashed arrows. For $B = 0$, the spectrum $E_k^0 = 2it \sin k$ (where $k \in [-\pi, \pi]$)

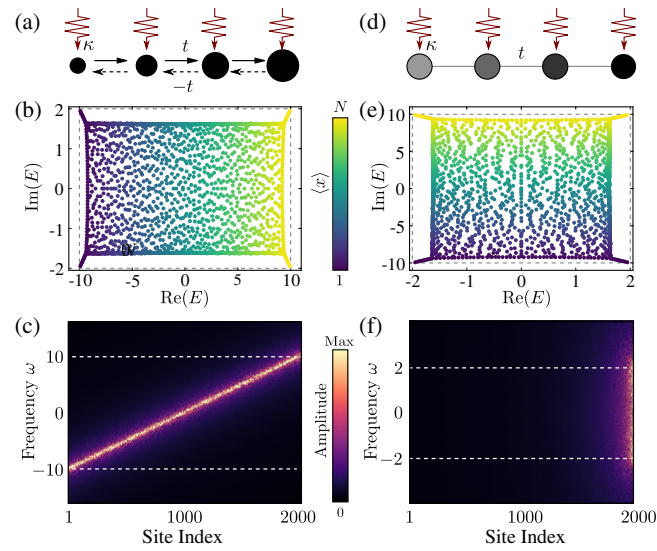


FIG. 3. Rainbow trapping and wave funneling in 1D lattices. (a) 1D lattice with nonreciprocal nearest neighbor hoppings of t (solid arrows) and $-t$ (dashed arrows). Each site j has real mass $m_j = B(j - j_0)$, where $j \in [1, N]$ and $j_0 = (N + 1)/2$. (b) Complex energy spectrum for the lattice in (a) with $N = 2000$, $t = 1$, and $B = 0.01$. The color of each dot indicates the eigenstate’s position expectation value $\langle x \rangle$. The dashed box shows the CLM energy bounds described in the text. (c) Site-dependent amplitudes under steady state excitation at frequency ω for the lattice in (b), with an additional per-site damping term $\Delta m = 1.9i$ to avoid blowup. On each site, the excitation has uniform amplitude but a random phase drawn uniformly from $[0, 2\pi)$. The two dashes show the working band $[-BN/2, BN/2]$. The peak position found to be proportional to ω . (d) 1D lattice with reciprocal nearest neighbor hopping t , and on-site mass $m_j = iB(j - j_0)$. (e) Complex energy spectrum for the lattice in (d) with $N = 2000$, $t = 1$, and $B = 0.01$. (f) Site-dependent amplitudes under the same excitation as in (c), using the lattice in (e) with additional per-site damping $\Delta m = 9.9i$. Dashes show the working band $[-2t, 2t]$. Funneling toward the large- j boundary is observed. In (c) and (f), the coupling of the excitation to each site is $\kappa = 0.2$.

is purely imaginary, lacking a point gap, and the lattice does not exhibit the non-Hermitian skin effect [43,44]. For $B \neq 0$, the effective Hamiltonian can be derived via the same procedures as in Eqs. (4)–(6):

$$H_k = E_k^0 + Bx + 2t \cos k \frac{\partial}{\partial x}. \quad (9)$$

This has CLM solutions [49] for $B/(t \cos k) < 0$ (i.e., k in half of the Brillouin zone). As in the 2D model, E takes any value in \mathbb{C} , but for finite N the eigenvalues reduce to a band as shown in Fig. 3(b), bounded by $|\text{Re}(E)| \lesssim BN/2$ and $|\text{Im}(E)| \lesssim 2t$. The bandwidth $\Delta[\text{Re}(E)] \sim BN$ is the detuning between the two end sites. The CLM center positions are $x_0 = \text{Re}(E)/B$ (independent of k , since E_k^0 is imaginary), consistent with the colors in Fig. 3(b).

Systems that have eigenstates localized at positions proportional to frequency can serve as “rainbow traps” [68–71], with potential applications in wave buffering and frequency demultiplexing. To demonstrate this, we apply a spatially incoherent monochromatic excitation $F(t) = e^{-i\omega t} \cdot [e^{i\theta_1}, \dots, e^{i\theta_N}]^T$, where each θ_j is a random initial phase. We then use the Green’s function to calculate the steady-state response [49,80]. As shown in Fig. 3(c), the response has a sharp amplitude peak positioned proportional to the excitation frequency. Previously studied rainbow traps have been based on Hermitian systems, and operate on different principles. The present scheme relies on the properties of the CLMs; when a comparable non-Hermitian lattice lacking CLMs is excited, the intensity peaks are distributed in different positions along the lattice with no evident relationship with frequency (see Supplemental Material [49]). The bandwidth $\Delta E \sim BN$ can be increased via the mass gradient B or lattice size N .

Another 1D lattice supporting CLMs, depicted in Fig. 3(d), has reciprocal hoppings along with a gradient in the on-site gain or loss. The Hamiltonian is

$$\mathcal{H} = \sum_j [iB(j - j_0)a_j^\dagger a_j + t(a_j^\dagger a_{j-1} + a_{j-1}^\dagger a_j)]. \quad (10)$$

For $B = 0$, this is Hermitian and the spectrum is $E_k^0 = 2t \cos k$. For $B \neq 0$, we obtain

$$H_k = E_k^0 + iBx + i2t \sin k \frac{\partial}{\partial x}. \quad (11)$$

There are CLM solutions [49] for $B/(t \sin k) < 0$. Figure 3(e) shows the spectrum for a finite lattice, which is bounded by $|\text{Re}(E)| \lesssim 2t$ and $|\text{Im}(E)| \lesssim BN/2$. As the CLMs are centered at $x_0 = \text{Im}(E)/B$, the modes with highest relative gain occur at a boundary. Under a spatially incoherent excitation, the steady-state response is concentrated at the boundary, as shown in Fig. 3(f). We emphasize that this is not simply due to the boundary site having the highest relative gain, since the funneling effect occurs over a bandwidth of $\Delta[\text{Re}(E)] \sim 4t$,

rather than the narrow linewidth of an isolated resonance. Similar funneling behavior has been associated with the non-Hermitian skin effect [36,37,40,41,43–46], but the present lattice does not exhibit the skin effect [49]. This way of implementing a wave funnel requires neither nonreciprocal hoppings nor complicated lattice symmetries. In Supplemental Material, we show that a similar lattice lacking CLMs does not induce funneling [49].

In conclusion, we have shown that a non-Hermitian Hamiltonian can host an uncountably infinite set of bound states, violating the intuition that bound states should be quantized. The bound states possess Gaussian envelopes and are related to zeroth Landau level modes [50–55]. We have shown how to implement these eigenstates in 1D and 2D lattices that are experimentally accessible via classical metamaterial platforms [46,61–67]. In 1D lattices, the linear relationship between position and energy allows for non-Hermitian rainbow trapping and light funneling functionalities. In future work, it would be interesting to determine the general conditions under which nonquantized bound states can arise, and to explore other ways to violate the distinction between bound and free states. Continuous families of bound states might emerge among other non-Hermitian systems unrelated to zeroth Landau level modes, with properties different from those studied here.

This work was supported by the Singapore MOE Academic Research Fund Tier 3 Grant No. MOE2016-T3-1-006 and Tier 1 Grant No. RG148/20, and by the National Research Foundation Competitive Research Programs NRF-CRP23-2019-0005 and NRF-CRP23-2019-0007.

*blzhang@ntu.edu.sg

†yidong@ntu.edu.sg

- [1] D. Ruelle, *Il Nuovo Cimento A* (1965–1970) **61**, 655 (1969).
- [2] W. O. Amrein and V. Georgescu, *Helv. Phys. Acta* **46**, 635 (1974).
- [3] W. Rudin, *Functional Analysis*, International series in pure and applied mathematics (McGraw-Hill, New York, 1991).
- [4] G. Teschl, *Grad. Stud. Math.* **99**, 106 (2009).
- [5] J. B. Conway, *A Course in Functional Analysis* (Springer, New York, 2019), Vol. 96.
- [6] L. D. Landau and E. M. Lifshitz, *Quantum Mechanics: Non-Relativistic Theory* (Elsevier, New York, 2013), Vol. 3.
- [7] J. Fröhlich and T. Spencer, *Phys. Rep.* **103**, 9 (1984).
- [8] D. Hundertmark, in *Analysis and Stochastics of Growth Processes and Interface Models*, edited by P. Mörters, R. Moser, M. Penrose, H. Schwetlick, and J. Zimmer (Oxford University Press, Oxford, 2008), Chap. 9, p. 194.
- [9] M. Lüscher, *Commun. Math. Phys.* **85**, 39 (1982).
- [10] K. Symanzik, *Nucl. Phys.* **B226**, 187 (1983).
- [11] C. Michael and M. Teper, *Phys. Lett. B* **199**, 95 (1987).
- [12] X.-G. Wen, *Int. J. Mod. Phys. B* **04**, 239 (1990).
- [13] E. McCann and V. I. Fal’ko, *Phys. Rev. Lett.* **96**, 086805 (2006).
- [14] Y. Zhang, Z. Jiang, J. P. Small, M. S. Purewal, Y.-W. Tan, M. Fazlollahi, J. D. Chudow, J. A. Jaszczak, H. L. Stormer, and P. Kim, *Phys. Rev. Lett.* **96**, 136806 (2006).
- [15] C. M. Bender and S. Boettcher, *Phys. Rev. Lett.* **80**, 5243 (1998).
- [16] A. Mostafazadeh, *J. Math. Phys. (N.Y.)* **43**, 205 (2002).
- [17] A. Mostafazadeh, *J. Math. Phys. (N.Y.)* **43**, 2814 (2002).
- [18] A. Mostafazadeh, *J. Math. Phys. (N.Y.)* **43**, 3944 (2002).
- [19] A. Mostafazadeh and A. Batal, *J. Phys. A* **37**, 11645 (2004).
- [20] Z. Gong, Y. Ashida, K. Kawabata, K. Takasan, S. Higashikawa, and M. Ueda, *Phys. Rev. X* **8**, 031079 (2018).
- [21] K. Kawabata, K. Shiozaki, M. Ueda, and M. Sato, *Phys. Rev. X* **9**, 041015 (2019).
- [22] E. J. Bergholtz, J. C. Budich, and F. K. Kunst, *Rev. Mod. Phys.* **93**, 015005 (2021).
- [23] A. Guo, G. J. Salamo, D. Duchesne, R. Morandotti, M. Volatier-Ravat, V. Aimez, G. A. Siviloglou, and D. N. Christodoulides, *Phys. Rev. Lett.* **103**, 093902 (2009).
- [24] C. E. Rüter, K. G. Makris, R. El-Ganainy, D. N. Christodoulides, M. Segev, and D. Kip, *Nat. Phys.* **6**, 192 (2010).
- [25] H. Hodaei, M.-A. Miri, M. Heinrich, D. N. Christodoulides, and M. Khajavikhan, *Science* **346**, 975 (2014).
- [26] L. Feng, Z. J. Wong, R.-M. Ma, Y. Wang, and X. Zhang, *Science* **346**, 972 (2014).
- [27] A. Schumer, Y. Liu, J. Leshin, L. Ding, Y. Alahmadi, A. Hassan, H. Nasari, S. Rotter, D. Christodoulides, P. LiKamWa, and M. Khajavikhan, *Science* **375**, 884 (2022).
- [28] W. Heiss, *J. Phys. A* **45**, 444016 (2012).
- [29] B. Zhen, C. W. Hsu, Y. Igarashi, L. Lu, I. Kaminer, A. Pick, S.-L. Chua, J. D. Joannopoulos, and M. Soljačić, *Nature (London)* **525**, 354 (2015).
- [30] Y. Xu, S.-T. Wang, and L.-M. Duan, *Phys. Rev. Lett.* **118**, 045701 (2017).
- [31] A. Cerjan, S. Huang, M. Wang, K. P. Chen, Y. Chong, and M. C. Rechtsman, *Nat. Photonics* **13**, 623 (2019).
- [32] M.-A. Miri and A. Alù, *Science* **363**, eaar7709 (2019).
- [33] H. Hodaei, A. U. Hassan, S. Wittek, H. Garcia-Gracia, R. El-Ganainy, D. N. Christodoulides, and M. Khajavikhan, *Nature (London)* **548**, 187 (2017).
- [34] W. Chen, Ş. Kaya Özdemir, G. Zhao, J. Wiersig, and L. Yang, *Nature (London)* **548**, 192 (2017).
- [35] M. P. Hokmabadi, A. Schumer, D. N. Christodoulides, and M. Khajavikhan, *Nature (London)* **576**, 70 (2019).
- [36] N. Hatano and D. R. Nelson, *Phys. Rev. Lett.* **77**, 570 (1996).
- [37] N. Hatano and D. R. Nelson, *Phys. Rev. B* **56**, 8651 (1997).
- [38] T. E. Lee, *Phys. Rev. Lett.* **116**, 133903 (2016).
- [39] F. K. Kunst, E. Edvardsson, J. C. Budich, and E. J. Bergholtz, *Phys. Rev. Lett.* **121**, 026808 (2018).
- [40] S. Yao and Z. Wang, *Phys. Rev. Lett.* **121**, 086803 (2018).
- [41] K. Yokomizo and S. Murakami, *Phys. Rev. Lett.* **123**, 066404 (2019).
- [42] D. S. Borgnia, A. J. Kruchkov, and R.-J. Slager, *Phys. Rev. Lett.* **124**, 056802 (2020).
- [43] N. Okuma, K. Kawabata, K. Shiozaki, and M. Sato, *Phys. Rev. Lett.* **124**, 086801 (2020).
- [44] K. Zhang, Z. Yang, and C. Fang, *Phys. Rev. Lett.* **125**, 126402 (2020).

- [45] K. Zhang, Z. Yang, and C. Fang, *Nat. Commun.* **13**, 2496 (2022).
- [46] S. Weidemann, M. Kremer, T. Helbig, T. Hofmann, A. Stegmaier, M. Greiter, R. Thomale, and A. Szameit, *Science* **368**, 311 (2020).
- [47] S. Longhi, *Ann. Phys. (Amsterdam)* **530**, 1800023 (2018).
- [48] B. Zhu, Q. Wang, D. Leykam, H. Xue, Q. J. Wang, and Y. D. Chong, *Phys. Rev. Lett.* **129**, 013903 (2022).
- [49] See Supplemental Material at <http://link.aps.org/supplemental/10.1103/PhysRevLett.130.103602> for quantization of bound states, mapping continuum Landau Modes to Zeroth Landau Level modes, time-dependent solutions, bound state continua in one dimensional models, derivation of effective Hamiltonian from lattice model, lattice eigenstates under open and periodic boundary conditions, calculation of steady-state solutions and behavior of Non-Hermitian lattices without CLMs.
- [50] N. M. R. Peres, F. Guinea, and A. H. Castro Neto, *Phys. Rev. B* **73**, 125411 (2006).
- [51] Y. Zhang, Z. Jiang, J. P. Small, M. S. Purewal, Y.-W. Tan, M. Fazlollahi, J. D. Chudow, J. A. Jaszczak, H. L. Stormer, and P. Kim, *Phys. Rev. Lett.* **96**, 136806 (2006).
- [52] K. Nomura and A. H. MacDonald, *Phys. Rev. Lett.* **96**, 256602 (2006).
- [53] F. Guinea, M. Katsnelson, and A. Geim, *Nat. Phys.* **6**, 30 (2010).
- [54] M. C. Rechtsman, J. M. Zeuner, A. Tünnermann, S. Nolte, M. Segev, and A. Szameit, *Nat. Photonics* **7**, 153 (2013).
- [55] H. Schomerus and N. Y. Halpern, *Phys. Rev. Lett.* **110**, 013903 (2013).
- [56] H. Shen and L. Fu, *Phys. Rev. Lett.* **121**, 026403 (2018).
- [57] M. Lu, X.-X. Zhang, and M. Franz, *Phys. Rev. Lett.* **127**, 256402 (2021).
- [58] K. Shao, Z.-T. Cai, H. Geng, W. Chen, and D. Y. Xing, *Phys. Rev. B* **106**, L081402 (2022).
- [59] X. Zhu, H. Wang, S. K. Gupta, H. Zhang, B. Xie, M. Lu, and Y. Chen, *Phys. Rev. Res.* **2**, 013280 (2020).
- [60] Y. Song, W. Liu, L. Zheng, Y. Zhang, B. Wang, and P. Lu, *Phys. Rev. Appl.* **14**, 064076 (2020).
- [61] T. Helbig, T. Hofmann, S. Imhof, M. Abdelghany, T. Kiessling, L. Molenkamp, C. Lee, A. Szameit, M. Greiter, and R. Thomale, *Nat. Phys.* **16**, 747 (2020).
- [62] D. Zou, T. Chen, W. He, J. Bao, C. H. Lee, H. Sun, and X. Zhang, *Nat. Commun.* **12**, 7201 (2021).
- [63] X. Zhang, Y. Tian, J.-H. Jiang, M.-H. Lu, and Y.-F. Chen, *Nat. Commun.* **12**, 5377 (2021).
- [64] L. Zhang, Y. Yang, Y. Ge, Y.-J. Guan, Q. Chen, Q. Yan, F. Chen, R. Xi, Y. Li, D. Jia, S.-Q. Yuan, H.-X. Sun, C. Hongsheng, and B. Zhang, *Nat. Commun.* **12**, 6297 (2021).
- [65] H. Gao, H. Xue, Z. Gu, L. Li, W. Zhu, Z. Su, J. Zhu, B. Zhang, and Y. Chong, *Phys. Rev. B* **106**, 134112 (2022).
- [66] Q. Liang, D. Xie, Z. Dong, H. Li, H. Li, B. Gadway, W. Yi, and B. Yan, *Phys. Rev. Lett.* **129**, 070401 (2022).
- [67] W. Wang, X. Wang, and G. Ma, *Nature (London)* **608**, 50 (2022).
- [68] K. L. Tsakmakidis, A. D. Boardman, and O. Hess, *Nature (London)* **450**, 397 (2007).
- [69] Q. Gan, Y. J. Ding, and F. J. Bartoli, *Phys. Rev. Lett.* **102**, 056801 (2009).
- [70] C. Lu, C. Wang, M. Xiao, Z. Q. Zhang, and C. T. Chan, *Phys. Rev. Lett.* **126**, 113902 (2021).
- [71] C. Lu, Y.-Z. Sun, C. Wang, H. Zhang, W. Zhao, X. Hu, M. Xiao, W. Ding, Y.-C. Liu, and C. Chan, *Nat. Commun.* **13**, 2586 (2022).
- [72] B. Peng, Ş. K. Özdemir, F. Lei, F. Monifi, M. Gianfreda, G. L. Long, S. Fan, F. Nori, C. M. Bender, and L. Yang, *Nat. Phys.* **10**, 394 (2014).
- [73] L. Chang, X. Jiang, S. Hua, C. Yang, J. Wen, L. Jiang, G. Li, G. Wang, and M. Xiao, *Nat. Photonics* **8**, 524 (2014).
- [74] H. Zhao, P. Miao, M. H. Teimourpour, S. Malzard, R. El-Ganainy, H. Schomerus, and L. Feng, *Nat. Commun.* **9**, 981 (2018).
- [75] H. Zhao, X. Qiao, T. Wu, B. Midya, S. Longhi, and L. Feng, *Science* **365**, 1163 (2019).
- [76] V. B. Berestetskii, E. M. Lifshitz, and L. P. Pitaevskii, *Quantum Electrodynamics: Volume 4* (Pergamon Press and Oxford 1982), Vol. 4.
- [77] K. Kawabata, K. Shiozaki, and S. Ryu, *Phys. Rev. Lett.* **126**, 216405 (2021).
- [78] M. M. Denner, A. Skurativska, F. Schindler, M. H. Fischer, R. Thomale, T. Bzdušek, and T. Neupert, *Nat. Commun.* **12**, 1 (2021).
- [79] D. J. Thouless, *Phys. Rep.* **13**, 93 (1974).
- [80] L. P. Kadanoff and G. Baym, *Quantum Statistical Mechanics: Green's Function Methods in Equilibrium and Nonequilibrium Problems* (CRC Press, Boca Raton, 2018).